Journal of Environmental Radioactivity 193–194 (2018) 82–90

Contents lists available at ScienceDirect

Journal of Environmental Radioactivity

journal homepage: www.elsevier.com/locate/jenvrad

Calibration of forest ^{137}Cs cycling model "FoRothCs" via approximate Bayesian computation based on 6-year observations from plantation forests in Fukushima

Kazuya Nishina[a,*], Shoji Hashimoto[b,d], Naohiro Imamura[b], Shinta Ohashi[b], Masabumi Komatsu[b], Shinji Kaneko[e], Seiji Hayashi[c]

[a] Center for Regional Environmental Research, National Institute for Environmental Studies, 305-8506, 16-2, Onogawa, Tsukuba, Ibaraki, Japan
[b] Forestry and Forest Products Research Institute, 305-8687, 1, Matsunosato, Tsukuba, Ibaraki, Japan
[c] Fukushima Branch, National Institute for Environmental Studies, 963-7700, 10-2, Fukasaku, Miharu, Fukushima, Japan
[d] The University of Tokyo, 113-8657, 1-1-1 Yayoi, Bunkyo-ku, Tokyo, Japan
[e] Kansai Research Center, Forestry and Forest Products Research Institute, 612-0855, 68, Nagaikyutaro, Momoyama, Fushimi, Kyoto, Japan

ARTICLE INFO

Keywords:
FoRothCs
Forest ecosystem
ABC-MCMC
^{137} Cs
Radioecology

ABSTRACT

Predicting the environmental fate of ^{137}Cs in forest ecosystems along with the concentrations of ^{137}Cs in tree parts are important for the managements of radioactively contaminated forests. In this study, we calibrate the Forest RothC and Cs model (FoRothCs), a forest ecosystem ^{137}Cs dynamics model, using observational data obtained over six years from four forest sites with different levels of ^{137}Cs contamination from Fukushima Prefecture. To this end, we applied an approximate Bayesian computation (ABC) technique based on the observed ^{137}Cs concentrations (Bq kg^{-1}) of five compartments (leaf, branch, stem, litter, and soil) in a Japanese cedar plantation. The environmental decay (increment) constants of the five compartments were used as the summary statistics (i.e., the metric for model performance) to infer the five parameters related to ^{137}Cs transfer processes in FoRothCs. The ABC technique successfully reconciled the model outputs with the observed trends in ^{137}Cs concentrations at all sites during the study period. Furthermore, the estimated parameters are in agreement with the literature values (e.g., the root uptake rates of ^{137}Cs). Our study demonstrates that model calibration with ABC based on the trends in ^{137}Cs concentrations of multi compartments is useful for reducing the prediction uncertainty of ^{137}Cs dynamics in forest ecosystems.

1. Introduction

The Fukushima Dai-ichi nuclear power plant (FDNPP) accident in March 2011 released 14.5 PBq of ^{137}Cs into the atmosphere (Katata et al., 2015), which resulted in its wide distribution over terrestrial environments in Japan mainly in the aerosol form (Morino et al., 2011; Katata et al., 2015). The dominant type in the area of land contaminated by the FDNPP accident is the forest ecosystem, which accounts for approximately 70% of the contaminated area and includes approximately 11 Mm^3 volume of aboveground biomass (Hashimoto et al., 2012). Radio-contaminated forest ecosystems in Japan primarily comprise plantation forests (e.g., Japanese cedar (*Cryptomeria japonica*) and red pine (*Pinus densiflora*)) for timber production. Even in steep Japanese forests, ^{137}Cs transport from the forest floor to the outer ecosystem has a relatively small contribution to total ^{137}Cs deposition in forest ecosystems (Niizato et al., 2016). Thus, understanding the long-term redistribution of ^{137}Cs in forest ecosystems is essential for managing contaminated forests and mitigating human and ecological impacts.

To facilitate management and ^{137}Cs decontamination in forest ecosystems, we developed a new open-source ^{137}Cs cycling model ("FoRothCs") that incorporates forest C cycling, including forest biomass production and soil C decomposition (Nishina and Hayashi, 2015). FoRothCs can simulate the dynamics of ^{137}Cs inventory (Bq m^{-2}) and of its concentrations (Bq kg^{-1}) in leaf, branch, stem, the litter, and soil compartments in monthly time steps. Recently, the mathematical models for forest ^{137}Cs cycling were also applied to the area contaminated by the FDNPP accident (e.g., Hashimoto et al., 2013; Nishina and Hayashi, 2015; Gonze and Calmon, 2017; Thiry et al., 2018). However, these models must be validated using observational

* Corresponding author.
E-mail address: nishina.kazuya@nies.go.jp (K. Nishina).

https://doi.org/10.1016/j.jenvrad.2018.09.002
Received 7 March 2018; Received in revised form 10 August 2018; Accepted 4 September 2018
Available online 13 September 2018

data before they are used to make long-term assessments (Shaw et al., 2005). Since the FDNPP accident occurred more than seven years ago, more time-series data on ^{137}Cs distributions in the forest ecosystems of Fukushima have recently become available (e.g., Komatsu et al., 2016; Imamura et al., 2017). Hence, more reliable model validation can be conducted in the area contaminated by FDNPP accident.

To improve prediction accuracy, calibrating models of forest ^{137}Cs cycling using observational ^{137}Cs fluxes would benefit instead of estimating the simple transfer factor coefficients (Goor and Thiry, 2004). Linkov et al. (1999) recommended a Bayesian calibration to reconcile forest ^{137}Cs model behavior based on observational data. This procedure reduces uncertainties in the parameter regarding ^{137}Cs transfer processes and enables the estimation of parameters that are difficult to measure in situ. In addition, this validation procedure reduces the uncertainty of projected ^{137}Cs redistribution in forest ecosystems (Linkov et al., 1999). However, model fitting based on multi-compartment ^{137}Cs datasets is inherently difficult due to the tree compartments having different orders of ^{137}Cs concentrations and its rates of transition. In addition, when calibrating a ^{137}Cs cycling model with multi-component of forest simultaneously, different units of measure are included. Because of different denominators in the unit for ^{137}Cs between plant and soil, the units of ^{137}Cs in plant tissues and soil are incomparable and should be distinguished even when using the same units (Bq kg^{-1}). Their concentrations should not be compared directly among different variables and therefore the cost function (or likelihood) is intractable in this case (e.g., Soetaert and Herman, 2008). In contrast, ecological half-life, a commonly used index of forest ^{137}Cs cycling (e.g., Pröhl et al., 2006; Calmon et al., 2009; Tagami and Uchida, 2015; Imamura et al., 2017), is comparable among compartments. To use this index as a measure of model accuracy, we adopted approximate Bayesian computation (ABC) (Beaumont et al., 2002) for model calibration; ABC enables making inferences with complex model parameters without likelihood (Csilléry et al., 2010). Hence, signature-based metrics can be easily incorporated as a summary statistics when using ABC for model evaluation (Vrugt and Sadegh, 2013).

To obtain more reliable simulations for ^{137}Cs cycling in forest ecosystems, we are developing a methodology to reconcile a forest ecosystem ^{137}Cs dynamics model to the observations. Assuming the multi-compartment information as a trend during 2011–2017, we applied an ABC method to reconcile the FoRothCs model with field data obtained from four sites in Fukushima Prefecture with different levels of ^{137}Cs contamination (Komatsu et al., 2016). This approach can be used to validate the FoRothCs model based on field observations and simultaneously infer the parameters related to ^{137}Cs migration that cannot be obtained directly from field observations.

2. Material & methods

2.1. Observation dataset

We used observations for six years of ^{137}Cs concentration datasets in Japanese cedar (*Cryptomeria japonica*) forests at four experimental sites with different levels of ^{137}Cs contamination (Komatsu et al., 2016) (Table 1). These data were provided by the Forestry and Forest Products Research Institute (FFPRI) and the Forestry Agency (Forestry agency, Japan, 2017) and are partially available in supplement material in Imamura et al. (2017). In this study, we used the "wood" data for ^{137}Cs (Imamura et al., 2017; Forestry agency, Japan, 2017) as "stem" data according to the definition of FoRothCs, which comprises sapwood and heartwood without bark compartment. We used ^{137}Cs concentrations in soil as top 20 cm depth in this study.

2.2. Model description and simulation settings

FoRothCs v1.0 (Nishina and Hayashi, 2015), which is coded in R (R Core Team, 2017), can simulate ^{137}Cs cycling and redistribution in forest ecosystems based on models of biomass production and C cycling in forest ecosystems. Carbon and biomass production in FoRothCs are modeled by the RothC model (Jenkinson et al., 1990) and the diameter distribution prediction system (DDPS) model (Hayashi et al., 2002), respectively. The RothC model is a carbon-cycling model for the decomposition of soil organic carbon, and DDPS is a self-thinning growth model for biomass production in managed forests. These two models are coupled in FoRothCs to model C cycling. Cs dynamics is incorporated into C cycling using transfer parameters. To summarize the overall model structure and transfer processes of FoRothCs, we used a matrix representation (Avila and Moberg, 1999) as in Fig. 1. The main model compartments are the leaf, branch, stem, litter, soil organic fraction, microbes, and soil mineral fraction (Fig. 1). The dynamics of ^{137}Cs in soil organic matter were based on the decomposition dynamics of the Roth-C model, and the allocation of ^{137}Cs to each soil compartments are according to Roth-C functions (Nishina and Hayashi, 2015). In this study, we summed the components of soil organic, microbe, and soil mineral compartments and treated it as a "soil" compartment. FoRothCs can predict ^{137}Cs inventory (Bq m^{-2}) and ^{137}Cs concentration (Bq kg^{-1} or Bq kg-C^{-1}) for each compartment given the following input variables and parameters: monthly climate data (temperature and precipitation), initial forest condition (stand age, tree density, and basal area), and parameters related to ^{137}Cs dynamics (e.g., ^{137}Cs deposition rate, initial ^{137}Cs inventory in each compartment, tree uptake rate "T_{uptake}", translocation rate "T_{uptake}", and pullback fraction "T_{uptake}"). T_{uptake} is a parameter that determines the uptake rate of ^{137}Cs relative to the ^{137}Cs in soil; this value is same for both organic soil and mineral soil compartments. T_{uptake} is the translocation parameter, which determines the fraction of ^{137}Cs that is recycled by green leaves before they become litterfalls. T_{uptake} determines the translocation rate from branches to leaves. Table 2 summarizes the input data and parameters of FoRothCs and Fig. 1 shows the structure of FoRothCs.

FoRothCs v1.1 was used in this study. This version is modified for seasonal tree growth (see code in Supplemental Material and Github) and it incorporates the throughfall migration of ^{137}Cs from tree crown to forest floor according to the double exponential (DE) model proposed

Table 1
General site descriptions (more detailed information is available in Imamura et al. (2017)).

	Kawauchi (KU)	Kamikawauchi (KU2)	Otama (OT)	Tadami (TD)
Latitude	37° 17′ 18″	37° 22′ 53″	37° 34′ 40″	37° 19′ 28″
Longitude	140° 47′ 48″	140° 42′ 58″	140° 18′ 20″	139° 31′ 15″
Elevation (m)	660	690	730	790
Annual mean air temperature† (°C)	10.7	10.7	11.8	9.9
Annual precipitation† (mm)	1574	1574	1176	2615
^{137}Cs deposition (kBq m^{-2})	688	283	54	11
Stand age in 2011 (year)	43	57	43	37
Tree density (trees ha^{-1})	975	733	1117	1105
Mean Diameter at Breast Height (cm)	18.8	30.9	24.8	19.9
Bulk soil density‡ (Mg m^{-3})	0.52	0.41	0.37	0.59

†; The data are averaged values over 2011–2015 at nearby meteorological stations KU, OT, and TD. ‡, for the top 20-cm layer.

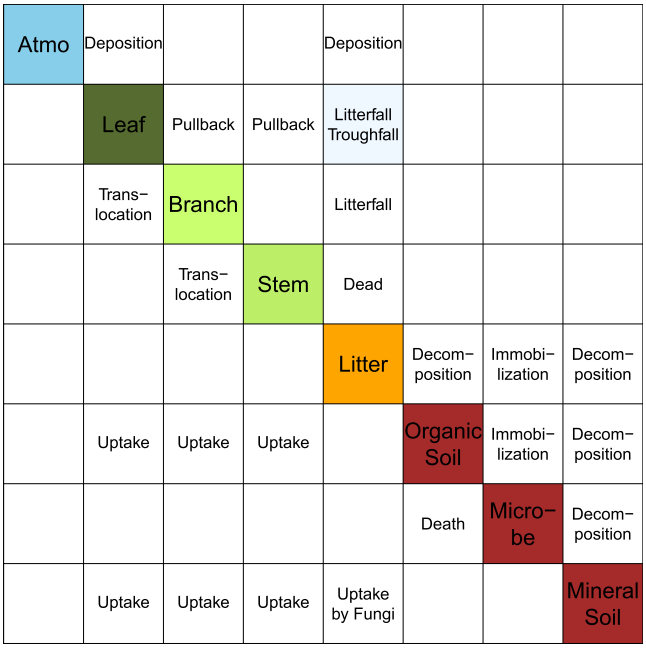

Fig. 1. Compartments and transfer processes in FoRothCs Ver. 1.1. Diagonal components indicate the compartment of FoRothCs. Other components indicate transfer processes among compartments. Each transfer process are defined in Nishina and Hayashi (2015).

Table 2
Input parameters for the FoRothCs model.

Element	Input variables and parameters	Unit	Abbreviation
All	Simulation duration from 2011	Year	Yr
	Latitude	°	Lat
Climate	Mean monthly temperature	°c	T
	Monthly precipitation	mm	P
Tree growth	Initial basal area (BA)	$M^2\ ha^{-1}$	BA_{in}
	Initial tree density (rho)	Trees ha^{-1}	ρ_{in}
	Stand age	Years	N_{in}
	Monthly litterfall fraction	%	Lit_{frac}
Soil	Target soil depth	cm	Dep
	Clay content	%	Clay
	Bulk density	Mg m^{-3}	BD
^{137}Cs cycling	Root uptake rate	$M^2\ kg^{-1}$ $month^{-1}$	T_{uptake}
	Translocation from branch to leaf	$Month^{-1}$	$T_{relocate}$
	Pullback fraction from leaf to branch	%	$T_{pullback}$
	Migration rate from soil to litter	kg_{soil} $month^{-1}$	L_{mig}
	Ratio of the slow to fast component of throughfall	–	R_{sf}
Management	Thinning rate	%	f_{thin}
	Thinning year	Year after deposition	Yr_{thin}
	Thinning month	Month	$Month_{thin}$
	Litter removal rate	%	f_{remove}
	Litter removal year	Year after deposition	Yr_{rm}
	Litter removal month	Month	$Month_{rm}$

by Loffredo et al. (2014, 2015). Throughfall was included because a large proportion of ^{137}Cs moves by throughfall during the early phase after the ^{137}Cs deposition (Gonze and Calmon, 2017; Kato et al., 2017). The DE model considers the fast and slow fractions of ^{137}Cs throughfall. The modified DE model (according to Wei et al. (2017)) was incorporated in FoRothCs v1.1 as follows:

$$TF_t = b_1 \mathbf{Pr}_t \mathbf{L}_t \frac{1}{1 + \frac{1}{R_{fs}}} \left(k_1 R_{fs} e^{-k_1 t} + k_2 e^{-k_2 t}\right) \quad (1)$$

where TF_t is monthly ^{137}Cs migration via throughfall (Bq m^{-2} $month^{-1}$), which depends on the amount of monthly precipitation "$\mathbf{Pr}_t$" (mm), the ^{137}Cs inventory (Bq m^{-2}) in the forest crown (leaf compartment) "$\mathbf{L}_t$", and the elapsed time after deposition t, which is monthly in FoRothCs; b_1 (mm^{-1}) is the sensitivity parameter against the amount of precipitation, which was set at 0.0172 mm^{-1} in this study based on an estimate for mature Japanese cedar forest (Loffredo et al., 2014); R_{fs} is the ratio of fast-loss fraction to slow-loss fraction for leachable ^{137}Cs in $\mathbf{L}_t$, which was set to 0.22 according to Loffredo et al. (2015); and k_1 and k_2 represent the kinetic parameters ($month^{-1}$) for each fast and slow fraction of the DE model, which were estimated by Loffredo et al. (2015) to be 5.0× 10^{-4} day^{-1} and 1.2× 10^{-4} day^{-1}, respectively.

For biomass production, we used the parameter of allometry equation estimated with the observation in these sites (Kajimoto et al., 2014) instead of the default value in FoRothCs v1.0. To obtain the initial values of soil organic carbon (soil organic layer), we ran a 1000-year simulation as a spin-up procedure in FoRothCs. In the spin-up procedure, we used the default parameter values, the initial forest condition (at the beginning of spin-up) and average climate conditions during 2011–2015 as a input variables. For the input of initial litter value in FoRothCs, we used maximum observed values reported by Imamura et al. (2017).

2.3. Model code availability

The model code of FoRothCs v1.1 is available in the Github repository (https://github.com/Nishina-NIES/FoRothCs). The original version of FoRothCs v1.0 is available in the supplementary information of Nishina and Hayashi (2015).

2.4. Parameter estimation using ABC

In this study, we applied ABC implemented with a Markov chain Monte Carlo (MCMC) algorithm (Marjoram et al., 2003); this approach is referred to as ABC-MCMC. The use of the MCMC algorithm reduces the ABC rejection rate. The ABC-MCMC scheme applied in this study is summarized as follows:

1. Initialize tolerance level ε and transition kernel $q(\theta'|\theta)$ according to the method by Wegmann et al. (2009).
2. Generate θ' from θ according to $q(\theta'|\theta)$.
3. Simulate FoRothCs using θ'.
4. Calculate a set of summary of statistics using the simulation results "$S(y')$".
5. if $d(S(y'), S(y_{obs})) < \varepsilon$, then go to 6. Otherwise, stay at θ and go to 2.
6. Accept the parameter θ' with probability $\min\left(1, \frac{\pi(\theta')q(\theta \mid \theta')}{\pi(\theta)q(\theta' \mid \theta)}\right)$. If not accept, stay at θ and go to 2.

The priors ($\pi(\theta)$) for θ are summarized in Table 3. We used uniform and log-uniform distribution, which is a uniform prior for the logarithm of the parameters ($f(x) = \{[\log_{10}(b) - \log_{10}(a)]x\}^{-1}$, $x \in [a, b]$), to the

Table 3
Priors for ^{137}Cs transfer parameters.

Parameter	Type of prior	Minimum	Maximum
T_{uptake}	Log-uniform	10^{-7}	10^{-2}
$T_{relocate}$	Log-uniform	10^{-5}	$10^{-0.5}$
$T_{pullback}$	Uniform	0	1
L_{mig}	Log-uniform	10^{-5}	10^{-1}
R_{sf}	Log-uniform	10^{-2}	10^{2}

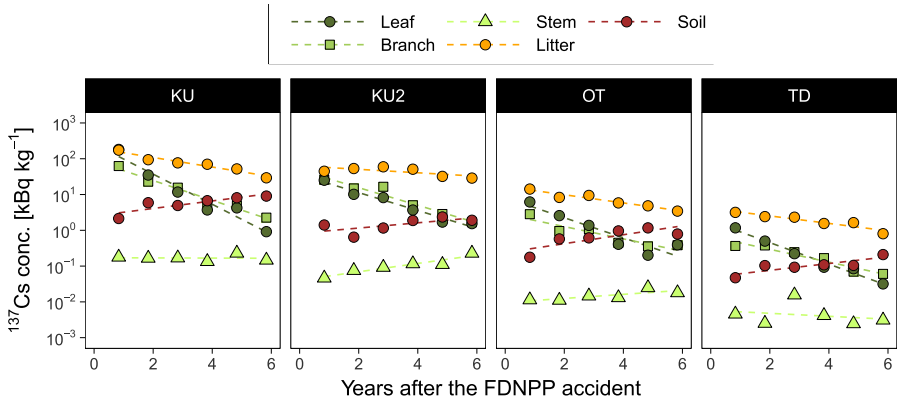

Fig. 2. Observed ^{137}Cs concentrations in each compartment at the four study sites. Circles indicate observations, and dotted lines indicate regression lines for each compartment. All observations are mean of three replicates.

priors. Detailed calibration process for ε and transition kernel $q(\theta'|\theta)$ is referred to Wegmann et al. (2009). "$S()$" indicates a vector of summary statistic. In this study, we used λ as a summary statistics, which is the environmental decay or increment (if positive) constant of the compartment and is defined as follows:

$$C(t)_i \sim \alpha_i e^{\lambda_i t} \tag{2}$$

where C(t) is ^{137}Cs concentration (Bq kg^{-1}) at time t (month) after the accident; i indicates the compartment (i = leaf, branch, stem, litter, soil); and α (Bq kg^{-1}) and λ (month^{-1}) are fitting parameters. In the case of negative values in λ, it is interpreted as the value of ecological half-lives "T_{ec}" (i.e., $\lambda = \ln 2/T_{en}$). For estimating λ to stabilize the estimation in the ABC procedure, we conducted linear regressions for each compartment after the logarithms of each concentrations against time (months after the FDNPP accident) in both observation and simulation results. $S(y_{obs})$ is summary statistics in the observation (Fig. 2; Table 4). For $S(y')$, we used simulation outputs with same sampling period of with the observation. In step 4, ε is the criteria for the acceptance of the simulation results in the Euclidean distance "d" between $S(y')$ and $S(y_{obs})$. ε is automatically determined from the algorithm of Wegmann et al. (2009) in the initial calibration step (step 1) in ABC-MCMC. To sample posterior, we obtained 10000 samples using MCMC; to avoid autocorrelation in chains, we set the thinning rate to be 10. ABC-MCMC was implemented in the R package "EasyABC" (Jabot et al., 2013) and R environment (R Core Team, 2017).

2.5. Assessing model error

To evaluate model performance, we calculated the mean absolute error (MAE) for each compartment and each site. These indices are defined as follows:

$$\mathrm{MAE}_i = \frac{1}{n}\sum_{k}^{n}\left|O_{i,k} - S_{i,k}\right| \tag{3}$$

where O_i and S_i are the observed and simulated ^{137}Cs concentrations (Bq kg^{-1}) in i compartment (i.e., leaf, branch, stem, litter, and soil), respectively. k indicates sampling periods and n indicates the number of samples in time-series (n = 6 in this study). To evaluate the ability of ABC-MCMC to improve model prediction, we also calculated MAE using the default model parameters and compared it to the MAE obtained with ABC-MCMC. To evaluate the improvement of the simulation, we calculated the relative changes in MAE between simulations with the default parameters "$\mathrm{MAE}_{default}$" and with the posterior medians "$\mathrm{MAE}_{posterior}$" as follows:

$$\Delta\mathrm{MAE}(\%) = \frac{\mathrm{MAE}_{posterior}}{\mathrm{MAE}_{default}} \times 100 \tag{4}$$

3. Results

3.1. Trends in ^{137}Cs concentrations in tree parts

We found that the ^{137}Cs concentrations in the leaf, branch, and litter layer exponentially decreased over time at all sites (Fig. 2) in agreement with the findings of a previous study based on five years of monitoring data (Imamura et al., 2017). Thus, the six years of observational data were generally well-fit using the linear models for log-transformed ^{137}Cs concentration in each compartment and site.

In leaves, the ecological half-lives ranged from 0.70 year at KU to

Table 4
λ for each compartment at each site.

Site	Parameter	Leaf	Branch	Stem	Litter	Soil
KU	λ	-8.98×10^{-2}	-5.30×10^{-2}	-0.52×10^{-2}	-2.56×10^{-2}	2.01×10^{-2}
	S.E. for λ	0.99×10^{-2}	0.43×10^{-2}	4.42×10^{-2}	0.33×10^{-2}	0.56×10^{-2}
	(T_{ec}†)	(0.71)	(1.09)		(2.25)	
KU2	λ	-4.91×10^{-2}	-4.89×10^{-2}	2.30×10^{-2}	-9.84×10^{-3}	1.47×10^{-2}
	S.E. for λ	0.52×10^{-2}	0.55×10^{-2}	0.38×10^{-2}	4.56×10^{-3}	0.78×10^{-2}
	(T_{ec}†)	(1.18)	(1.16)		(5.87)	
OT	λ	-5.37×10^{-2}	-3.29×10^{-2}	1.10×10^{-2}	-2.19×10^{-2}	2.39×10^{-2}
	S.E. for λ	1.12×10^{-2}	0.71×10^{-2}	0.41×10^{-2}	0.29×10^{-2}	0.90×10^{-2}
	(T_{ec}†)	(1.08)	(1.76)		(2.64)	
TD	λ	-5.77×10^{-2}	-3.43×10^{-2}	-0.79×10^{-2}	-2.01×10^{-2}	1.82×10^{-2}
	S.E. for λ	0.46×10^{-2}	0.48×10^{-2}	1.48×10^{-2}	0.37×10^{-2}	0.54×10^{-2}
	(T_{ec}†)	(1.00)	(1.68)		(2.87)	

The unit for λ is month^{-1}. †; T_{ec} indicate ecological half-life (year).

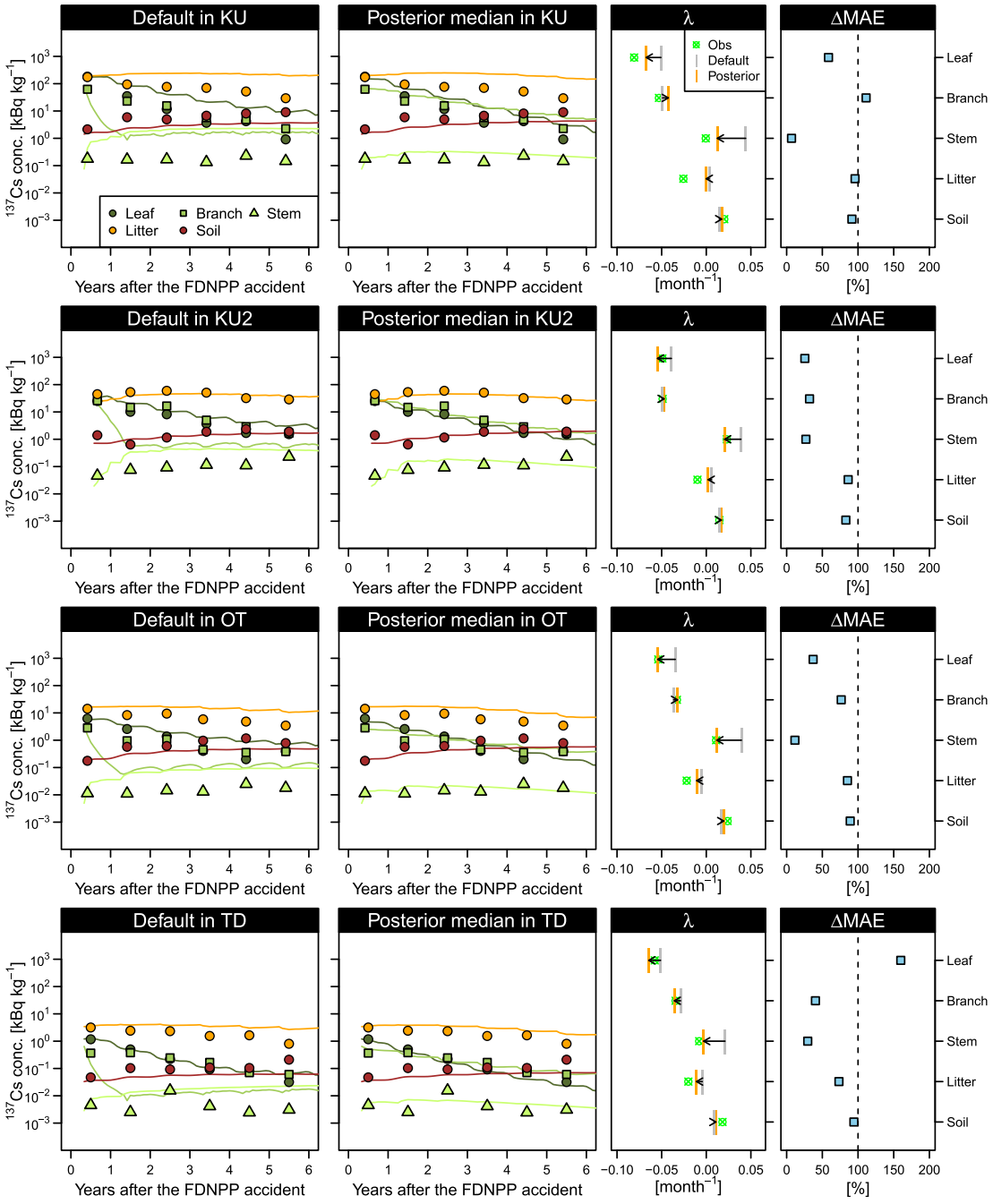

Fig. 3. FoRothCs simulation results for each site with the default parameter sets (left-most column) and posterior medians (second column). The third column shows the observed and simulated λ for each compartment (eq. (2)). The right-most column shows ΔMAE, that is the relative changes in MAE (eq. (4)). In the two left columns, circles indicate observed values, and lines indicate FoRothCs simulation output using the default parameters (left-most column) and posteriors (second column). The arrows in the third column indicate differences in λ between the default simulations and posterior simulations.

1.16 year at KU2. λ_{stem} varied from -7.94×10^{-3} month^{-1} to 2.30×10^{-2} month^{-1} (Table 4). Positive λ_{stem} values were observed at the KU2 and OT sites. Compared with λ in the two aboveground compartments (leaf and branch), λ_{litter} was smaller at all sites (Fig. 2, Table 4), suggesting that ^{137}Cs is persistent in the litter layer (2.22–5.51 year). In soil, ^{137}Cs concentration generally increased with time at all sites because of ^{137}Cs migration from the aboveground compartments (Fig. 2). The estimated λ_{soil} varied from 1.47×10^{-2} month^{-1} to 2.39×10^{-2} month^{-1} (Table 4).

3.2. Updating parameters using ABC

To obtain posteriors, the values of ε, which is the threshold for the acceptance by initializing in step 1, in ABC-MCMC were 21.8 in KU, 0.99 in KU2, 0.02 in OT, and 0.56 in TD. The highest ε might be attributed to the relatively large difference in λ of litter compartment.

Compared to the use of the default parameters, the use of the posterior median in the simulations improved the accuracy of λ in almost all compartments and sites with a few exceptions (λ_{branch} in KU, Fig. 3). This suggests that ABC-MCMC successfully improved the accuracy of simulated half-lives in individual compartments. While the ABC-MCMC fitting procedure also improved the MAE in most compartments (i.e.,

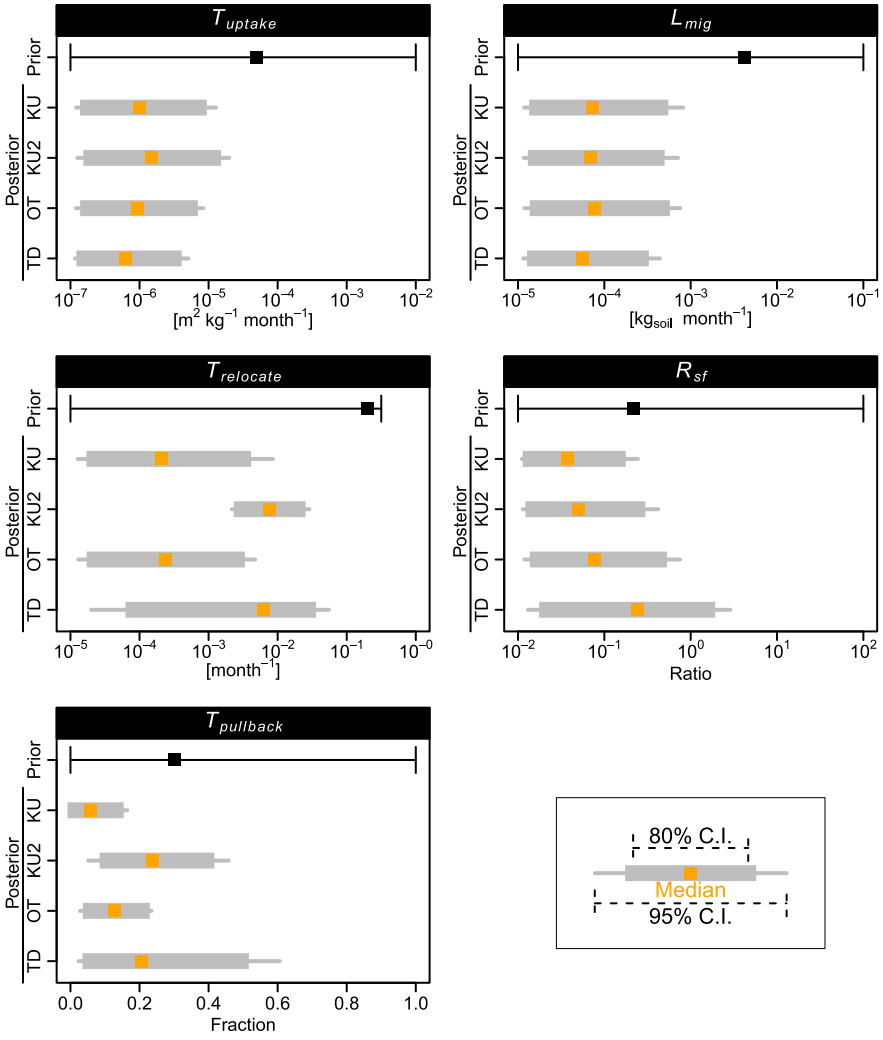

Fig. 4. Posterior distributions of T_{uptake}, $T_{pullback}$, $T_{relocate}$, L_{mig}, and R_{sf}. T_{uptake} indicate root uptake rate. $T_{pullback}$ indicate pullback fraction from leaf to branch. $T_{relocate}$ indicate translocation from branch to leaf. L_{mig} indicate migration rate from soil to litter. R_{sf} indicate ratio of the slow to fast component of throughfall. C.I. indicates credible interval.

decrease in ΔMAE in Fig. 3), using the posterior median worsened the MAE in some compartments compared to the use of the default parameters. For example, the posterior MAE was slightly greater than the original MAE for the branch compartment at KU. The largest ΔMAE was found in the leaf compartment at TD, whose value was 160%. However, even in the posterior simulation, MAE was sufficiently small (0.045 kBq kg^{-1}).

For the root uptake of ^{137}Cs "T_{uptake}", the posteriors medians were similar among the four sites; however, the T_{uptake} in KU2 (1.46×10^{-6} m^2 kg^{-1} month^{-1}) was the highest in the posterior medians among the sites (Fig. 4). But even in KU2, posterior medians of T_{uptake} were lesser than the default value. $T_{relocate}$ ranged from 1.83×10^{-4} month^{-1} (in OT) to 5.70×10^{-3} month^{-1} (in TD). The posterior median $T_{pullback}$ ranged from 5.7% to 26.9%. Among the four sites, KU exhibited the highest $T_{pullback}$ (26.9%) followed by TD (17.2%). The $T_{pullback}$ values at the remaining two sites were approximately 5%.

The posterior median L_{mig} values were similar among the sites (range; 5.56×10^{-5} month^{-1} to 7.77×10^{-5} month^{-1}), while the values were smaller than the default values by two orders of magnitude. The L_{mig} value for KU2 was comparable to the default value derived from an incubation study (Fukuyama and Takenaka, 2004).

The posterior median R_{sf} values varied from 0.05 (in KU) to 0.38 (in TD), indicating a slow fraction of 5.3%–27.5% against the intercepted ^{137}Cs in forest crown (leaf compartment). The order in posterior median R_{sf} values was reversed to the order in the initial amount of ^{137}Cs deposition (Table 1).

4. Discussion

4.1. Model fitting and diagnostic evaluation of posterior simulation

The ABC-MCMC approach generally improved the accuracy of FoRothCs at all sites (right-most panels in Fig. 3) and allowed the determination of parameters related to ^{137}Cs transfer (Fig. 4). The simulations using the default parameters clearly failed to capture ^{137}Cs dynamics in the branch and stem compartments at all sites (Fig. 3), indicating that the default parameter sets are not optimal for ^{137}Cs dynamics in Japanese cedar. The default parameters in FoRothCs (Nishina and Hayashi, 2015) were originally obtained by referring to the aggregated transfer factor T_{ag}, which is the ratio of the radionuclide concentration in plant divided by the total inventory on the soil per unit area, for coniferous species in literature review (Calmon et al., 2009) using grid-searching methods, a basic optimization method. In contrast, the simulations using the posterior medians accurately reproduced the observed trends in ^{137}Cs concentrations (Fig. 3). This indicates that ABC, which is similar to the full Bayesian approach (Linkov et al., 1999) but is easier to apply, allowed us to reconcile the model predictions with the field data. From application of the ABC approach, considerable

variations in the posteriors were found among sites (Fig. 4). Environmental differences in forest ecosystems result in inherent uncertainty and variability in radioecological cycling (Linkov et al., 1999); thus, data-assimilation approaches based on mathematical models and site-specific observations might be useful to understand intermediate to long-term ^{137}Cs redistribution in forest ecosystems.

Applying summary statistics for parameter inference is one of the advantages of the ABC approach (Vrugt and Sadegh, 2013). For parameter inference, we used a set of λ (i.e., a coefficient of exponential function) as a summary statistic in ABC-MCMC. This is because, for the parameter inference in this study, it is difficult to deal the multi-compartment concentrations, which have different digits orders of initial ^{137}Cs concentrations and changes even during 2011–2016. For example, the ^{137}Cs concentration of leaf at KU decreased from 183 to 0.92 kBq kg^{-1} during this period (Fig. 2), whereas the ^{137}Cs concentration in stem at KU remained stable at approximately 0.17 kBq kg^{-1} during the same period. In this case, the weight of the cost function for the fitting procedure must be carefully selected. In our approach, the use of λ as a summary statistic makes it easy to account for the dynamics in all compartments in the similar orders of magnitude (Table 4, Fig. 3). This improved the prediction accuracy for all compartments in our dataset and model. As λ (i.e., ecological half-life) is a commonly used parameter in radioecology, it is readily available for various forest ecosystems and could be a useful index for model validation.

Although fitting the model to data in this study improved both the trends in ^{137}Cs concentration (as evaluated by λ) and in general the ^{137}Cs concentrations themselves as evaluated by MAE (Fig. 3), the fitting procedure had only slight effects on λ and MAE in the litter and soil compartments at three sites. Furthermore, posterior simulation increases the value of MAE in the leaf compartment in TD and in the branch compartment in KU compared to simulation wherein the default parameters are used (Fig. 3). Thus, in some case, the improvement of some compartments resulted in the decreasing or hardly improving the fitness of model in other compartments due to the satisfying mass balance among the compartments in the model. Nevertheless, our approach might have advantages in the fundamental model improvement owing to the following reasons. MAE in leaf compartment in TD was still small even in the posterior simulation (0.043 kBq kg^{-1} in posterior simulation and 0.027 kBq kg^{-1} in default simulation). At the site KU, the branch simulations with default parameters did not apparently reproduce the observational data in KU. In this site, the regression for λ in these cases was obviously inadequate; however, the branch simulations with posterior was apparently succeeded to follow the observation. In the light to litter and soil compartments, the fitting procedure does not include any active adjustment using soil-related parameters. This is another reason why MAE were not drastically improved in these two compartments.

4.2. Transfer processes

The amount of initial ^{137}Cs deposition clearly determined the site-to-site differences of the initial ^{137}Cs concentrations of each compartments (Komatsu et al., 2016). In contrast, the estimated parameters (posterior medians), i.e., the rates of transfer of ^{137}Cs showed no clear dependency with initial ^{137}Cs deposition of each site instead of R_{sf}. Ohashi et al. (2017) reported that no obvious linear relationships in the trends of ^{137}Cs concentrations against the amount of initial deposition in the stems of Japanese cedar and Hinoki cypress (*Chamaecyparis obtusa*, the second most common conifer species on plantations in Japan) with respect to the initial level of contamination. As all transfer processes are inter-connected (Fig. 1), the comprehensive parameter inference is essential to reveal differences in ^{137}Cs cycling and trends. Thus, also as a posterior checking, we discuss the transfer processes by the fitted parameter values in the following paragraphs.

The values of $T_{relocate}$ and $T_{pullback}$ were higher at KU2 and TD than at the other two sites, suggesting that internal ^{137}Cs recycling might be an important mechanism of maintaining ^{137}Cs concentration in these forest stands, even though the difference in $T_{relocate}$ among the sites were still not apparent due to the large 95% credible intervals (C.I.) in the posterior of $T_{relocate}$ in three sites (except KU2). Previous field studies demonstrated that internal ^{137}Cs recycling is essential flux in forest ecosystems (Thiry et al., 2002, 2016; Rantavaara et al., 2012; Nishikiori et al., 2015). A significant fraction of ^{137}Cs that is intercepted by forest crown might be absorbed by leaves and partially absorbed by the plant tissue (Nishikiori et al., 2015; Thiry et al., 2016). The direct absorption of ^{137}Cs by tree surfaces has important effects on both the initial ^{137}Cs concentrations in trees and the long-term ^{137}Cs dynamics (Mahara et al., 2014). In this study, the estimated values of $T_{pullback}$ were less than 28.3%. An experiment on spruce trees (Thiry et al., 2016) found that 30% of stable Cs deposited on leaves was transferred to other compartments. In a study on Japanese cedar (Nishikiori et al., 2015), 20–40% of total ^{137}Cs was found inside leaves as a results of leaf surface uptake of the initial deposited ^{137}Cs. Furthermore, based on the ratio of stable Cs to ^{137}Cs in the sprouted leaves of Japanese cedar, Nishikiori et al. (2015) found that ^{137}Cs inside leaves can easily migrate to the other compartment. Thus, the posterior median values of $T_{pullback}$ would be realistic.

Cesium-137 uptake via roots is also an important process for the long-term dynamics of ^{137}Cs concentration of tree parts (e.g., Calmon et al., 2009; Thiry et al., 2018). Thus, estimating the ^{137}Cs uptake rates of trees in contaminated forest is critical for the decadal-scale prediction of ^{137}Cs concentration in the trees. In this study, T_{uptake} varied from 0.58×10^{-6} to 1.45×10^{-6} m^2 kg^{-1} month^{-1}. The transfer factor is known to vary widely by two to three orders of magnitude depending on the environment even within the same species (Calmon et al., 2009). Thus, the differences observed in this study might be acceptable, even though T_{uptake} was estimated indirectly using a model fitting approach. In the light of the differences in T_{uptake} among sites, the high estimated T_{uptake} for KU2 was consistent with the high transfer factor for stable Cs (^{137}Cs concentration in leaf/exchangeable ^{137}Cs in soil) reported in preceding study in the same sites (Nagakura et al., 2016). Because the in situ evaluation of ^{137}Cs uptake rate (flux) in roots requires extensive field works, few studies have assessed the uptake rate of ^{137}Cs into the roots of trees. Recently, Yoschenko et al. (2017) evaluated T_{uptake} in a Japanese cedar forest (43 years old) based on the annual biomass production, which value can be transformed T_{uptake} to be 9.06×10^{-6} m^2 kg^{-1} month^{-1}. For a forest of Scot pine (57 years old) in a Chernobyl-contaminated area, T_{uptake} was 1.15×10^{-6} m^2 kg^{-1} month^{-1}. These literature values are comparable to the T_{uptake} estimated in this study. A field transplanting experiment study of three-year-old, ^{137}Cs-free Hinoki cypress seedlings (Komatsu et al., 2017) found tree uptake rates (T_{uptake}) of 3.80×10^{-5} m^2 kg^{-1} month^{-1} in leaves and 4.81×10^{-5} m^2 kg^{-1} month^{-1} in stems (or 4.35×10^{-5} m^2 Bq^{-1} in the tree as a whole, greater than our estimated value). Generally, the rate of ^{137}Cs uptake via roots is lower in mature wood than in young trees (e.g., Thiry et al., 2002; Goor and Thiry, 2004; Shaw, 2007). Thus, tree age is a potential factor regulating ^{137}Cs uptake in trees. However, tree age was likely insignificant in this study as there were only small differences in tree age among the four study sites. Further improvements for the tree age-dependent migration rate are needed in FoRothCs.

The migration of ^{137}Cs via root uptake is implemented in FoRothCs as a simple function based on the aggregate transfer factor T_{ag}. In general, ^{137}Cs in soils become less bioavailable with time due to the fixation to clay minerals (e.g., Frissel, 1996; Kirchner, 1998; Rigol et al., 2002; Spiridonov et al., 2005; Ota et al., 2016; Beresford et al., 2016). Thus, ^{137}Cs uptake rates are typically modeled as a time-dependent parameter. In some modeling studies (Spiridonov et al., 2005; Ota et al., 2016), ^{137}Cs is modeled as different forms in the soil with different availabilities for plant absorption. Rigol et al. (2002) reported that soil organic matter indirectly decreased the Cs solid-liquid distribution coefficient, thereby enhancing the soil-to-plant transfer of Cs. These processes affect the root uptake rate of ^{137}Cs and are particularly

important on the decadal time scale of ^{137}Cs migrations. However, to implement detailed soil processes into the model, the soil compartment must be extensively parameterized. Currently, hardly any data are available on the speciation of ^{137}Cs forms in soils in Fukushima; thus, it remains difficult to infer time-dependent T_{uptake} using ABC because of the drastic changes in soil ^{137}Cs inventory caused by the loss of Cs from the canopy in this early phase (Coppin et al., 2016). Long-term monitoring and detailed information on the forms of ^{137}Cs in soil will improve our understanding of ^{137}Cs migration processes in soil.

Upward migration rate of ^{137}Cs from the soil to the litter (L_{mig}) might have been underestimated in this study. Previous reports suggest that the upward ^{137}Cs migration by microbes from soil to the litter layer might cause the ^{137}Cs concentration to remain high in the litter layer (Brückmann and Wolters, 1994; Fukuyama and Takenaka, 2004; Huang et al., 2016). In this study, the estimated L_{mig} values were one to two orders of magnitude smaller than the default values determined based on an incubation experiment involving different conifer species in Japan (Fukuyama and Takenaka, 2004) (Fig. 4). A recent six-month field litter-bag experiment on deciduous oak litter layer (Huang et al., 2016) found a L_{mig} of approximately $2.3\times 10^{-2}\,kg_{soil}\,month^{-1}$, which was greater than the default value in FoRothCs. Even when using posteriors, the simulated ^{137}Cs concentration in litter compartment did not agree with the observed values for the sites KU and OT (Fig. 3). In FoRothCs, the transfer of ^{137}Cs from litter to the soil compartment is modeled as migration accompanied by litter decomposition (Nishina and Hayashi, 2015) (Fig. 1). However, in situ, ^{137}Cs transfer from litter layer to soil via water infiltration is also an important process (Nakanishi et al., 2014; Takada et al., 2016; Iwagami et al., 2017). Iwagami et al. (2017) suggested that ^{137}Cs migration via water seepage at the soil surface involves slow and fast fractions, similar to ^{137}Cs migration from the canopy to the forest floor via throughfall. Not considering the fast migration process could lead to the underestimation of litter layer to soil migration rates and thus underestimation of L_{mig} in this study. To infer more realistic parameter value of L_{mig} from field study, FoRothCs requires the improvement of the migration processes in litter layer and more detailed observations for more specific fluxes.

The correlation between the posterior median values of the ratio of slow to fast components in throughfall migration "R_{sf}" with the initial deposition rates (Table 1 and Fig. 4) should be carefully examined. The posterior R_{sf} values in this study are comparable with previous reports on Japanese cedar forests and other coniferous forests (Loffredo et al., 2014, 2015; Thiry et al., 2016; Kato et al., 2017). However, the posterior R_{sf} values in this study had large uncertainties and exhibited significant overlap among the four sites. This can be attributed to the weak identifiability of this parameter because no data on throughfall migration rates were available. Thus, the observed correlation should be considered unreliable until it can be verified with additional field data.

In this study, we successfully reconciled FoRothCs outputs to the independent observation in four different sites using ABC-MCMC. The posteriors generally showed similar order of value among the sites. These results suggested that FoRothCs might have sufficient structure to simulate the forest ^{137}Cs dynamics in Japanese cedar forest, even though there exists some process uncertainties as discussed above and reviewed in detail by Diener et al. (2017). Provided that further validation is required for the other forest types and different site, FoRothCs could be useful tool to predict ^{137}Cs redistribution in plantation forests and evaluate their risks of forestry and decontamination managements (Nishina and Hayashi, 2015). Finally, our calibration approach could be useful for the other forest radioecological models.

5. Conclusion

Using an ABC approach, we calibrated the forest ^{137}Cs cycling model FoRothCs based on six years of observational data from four Japanese cedar forest sites in Fukushima. After model calibration, the model simulations and observations showed good agreement. This study demonstrates that the ABC approach based on trends in ^{137}Cs concentration is useful to improve the prediction accuracy of radioecological models and to infer the associated parameters. Updating radioecological models based on observed trends of ^{137}Cs concentrations also provides physiological insights related to ^{137}Cs cycling in forest ecosystems. Because ABC is flexible and relatively easy to implement (Csilléry et al., 2010; Vrugt and Sadegh, 2013), this approach can be applied in other modeling studies for ^{137}Cs cycling in forest ecosystems.

Extensive data including biomass measurements are required to evaluate transfer processes in forest ecosystems using field surveys (Yoschenko et al., 2017). Furthermore, Yoschenko et al. (2017) reported that estimates of ^{137}Cs uptake into tree roots based on field data have inherent uncertainty. In contrast, model assimilation approaches require only the changes in ^{137}Cs concentrations in individual compartments to estimate ^{137}Cs flux. Thus, calibrating mathematical models with field data shows promise for understanding ^{137}Cs dynamics in forest ecosystems.

To model the forest contaminated by the Chernobyl accident, IAEA's BIOMASS Forest Working Group compared 10 different models based on eight years of observational data collected in Ukraine (Shaw et al., 2005). This model inter comparison study suggested that the dominant source of uncertainty in the prediction of ^{137}Cs dynamics was attributed to the different model structures. To evaluate the uncertainty in the prediction of ^{137}Cs cycling, model inter-comparison study accompanied with data-model fusion approach, such ABC, is essential for future research.

Declaration of interest statement

There are no conflicts of interest to declare.

Acknowledgement

We appreciate Dr. T. Matsuura of FFPRI for valuable comments on this paper. We appreciate Dr. K. Fukasawa of NIES for valuable feedback related to posterior evaluation. This study was supported by MEXT research grants "16H04945" and "16H01791".

Appendix A. Supplementary data

Supplementary data related to this article can be found at https://doi.org/10.1016/j.jenvrad.2018.09.002.

References

Avila, R., Moberg, L., 1999. A systematic approach to the migration of ^{137}Cs in forest ecosystems using interaction matrices. J. Environ. Radioact. 45, 271–282. https://doi.org/10.1016/S0265-931X(98)00111-8.

Beaumont, M.A., Zhang, W., Balding, D.J., 2002. Approximate bayesian computation in population genetics. Genetics 162, 2025–2035.

Beresford, N., Fesenko, S., Konoplev, A., Skuterud, L., Smith, J., Voigt, G., 2016. Thirty years after the Chernobyl accident: what lessons have we learnt? J. Environ. Radioact. 157, 77–89. https://doi.org/10.1016/j.jenvrad.2016.02.003.

Brückmann, A., Wolters, V., 1994. Microbial immobilization and recycling of ^{137}Cs in the organic layers of forest ecosystems: relationship to environmental conditions, humification and invertebrate activity. Sci. Total Environ. 157, 249–256. https://doi.org/10.1016/0048-9697(94)90586-X.

Calmon, P., Thiry, Y., Zibold, G., Rantavaara, A., Fesenko, S., 2009. Transfer parameter values in temperate forest ecosystems: a review. J. Environ. Radioact. 100, 757–766. https://doi.org/10.1016/j.jenvrad.2008.11.005.

Coppin, F., Hurtevent, P., Loffredo, N., Simonucci, C., Julien, A., Gonze, M.A., Nanba, K., Onda, Y., Thiry, Y., 2016. Radiocaesium partitioning in Japanese cedar forests following the early phase of Fukushima fallout redistribution. Sci. Rep. 6, 37618. https://doi.org/10.1038/srep37618.

Csilléry, K., Blum, M.G., Gaggiotti, O.E., François, O., 2010. Approximate bayesian computation (ABC) in practice. Trends Ecol. Evol. 25, 410–418. https://doi.org/10.1016/j.tree.2010.04.001.

Diener, A., Hartmann, P., Urso, L., i Batlle, J.V., Gonze, M., Calmon, P., Steiner, M., 2017. Approaches to modelling radioactive contaminations in forests–Overview and

guidance. J. Environ. Radioact. 178, 203–211. https://doi.org/10.1016/j.jenvrad.2017.09.003.
Forestry agency, Japan, 2017. Present State of Forest Resources. (last access; 9, August, 2017). Forestry agency, Japan. URL. http://www.rinya.maff.go.jp/j/kaihatu/jyosen/H28/jittaihaaku/kekka.html.
Frissel, M.J., 1996. Soils role in the restoration of terrestrial sites contaminated with radioactivity. In: Luykx, F.F., Frissel, M.J. (Eds.), Radioecology and the Restoration of Radioactive-contaminated Sites. Springer Netherlands, Dordrecht, pp. 85–102. https://doi.org/10.1007/978-94-009-0301-2_8.
Fukuyama, T., Takenaka, C., 2004. Upward mobilization of ^{137}Cs in surface soils of Chamaecyparis obtusa Sieb. et Zucc. (hinoki) plantation in Japan. Sci. Total Environ. 318, 187–195. https://doi.org/10.1016/S0048-9697(03)00366-8.
Gonze, M.A., Calmon, P., 2017. Meta-analysis of radiocesium contamination data in Japanese forest trees over the period 2011–2013. Sci. Total Environ. 601, 301–316. https://doi.org/10.1016/j.scitotenv.2017.05.175.
Goor, F., Thiry, Y., 2004. Processes, dynamics and modelling of radiocaesium cycling in a chronosequence of Chernobyl-contaminated Scots pine (*Pinus sylvestris* L.) plantations. Sci. Total Environ. 325, 163–180. https://doi.org/10.1016/j.scitotenv.2003.10.037.
Hashimoto, S., Matsuura, T., Nanko, K., Linkov, I., Shaw, G., Kaneko, S., 2013. Predicted spatio-temporal dynamics of radiocesium deposited onto forests following the Fukushima nuclear accident. Sci. Rep. 3. https://doi.org/10.1038/srep02564.
Hashimoto, S., Ugawa, S., Nanko, K., Shichi, K., 2012. The total amounts of radioactively contaminated materials in forests in Fukushima, Japan. Sci. Rep. 2, 416. https://doi.org/10.1038/srep00416.
Hayashi, T., Yamamoto, K., Umemura, T., 2002. A system to predict diameter distribution in pure even-aged Hinoki (*Chamaecyparis obtusa* Sieb.) plantations (i): diameter distribution prediction system. J. Forest Plan. 8, 31–39. https://doi.org/10.20659/jfp.8.2_31.
Huang, Y., Kaneko, N., Nakamori, T., Miura, T., Tanaka, Y., Nonaka, M., Takenaka, C., 2016. Radiocesium immobilization to leaf litter by fungi during first-year decomposition in a deciduous forest in Fukushima. J. Environ. Radioact. 152, 28–34. https://doi.org/10.1016/j.jenvrad.2015.11.002.
Imamura, N., Komatsu, M., Shinta, O., Shoji, H., Kajimoto, T., Kaneko, S., Takano, T., 2017. Temporal changes in the radiocesium distribution in forests over the five years after the Fukushima Daiichi Nuclear Power Plant accident. Sci. Rep. 7, 416. https://doi.org/10.1038/s41598-017-08261-x.
Iwagami, S., Onda, Y., Tsujimura, M., Hada, M., Pun, I., 2017. Vertical distribution and temporal dynamics of dissolved ^{137}Cs concentrations in soil water after the Fukushima Dai-ichi Nuclear Power Plant accident. Environ. Pollut. 230, 1090–1098. https://doi.org/10.1016/j.envpol.2017.07.056.
Jabot, F., Faure, T., Dumoulin, N., 2013. EasyABC: performing efficient approximate bayesian computation sampling schemes using R. Meth. Ecol. Evol. 4, 684–687. https://doi.org/10.1111/2041-210X.12050.
Jenkinson, D., Andrew, S., Lynch, J., Goss, M., Tinker, P., 1990. The turnover of organic carbon and nitrogen in soil. Philos. T. R. Soc. Lond. B. 329, 361–368.
Kajimoto, T., Takano, T., Saito, S., Kuroda, K., Fujiwara, T., Komatsu, M., Kawasaki, T., Ohashi, S., Kiyono, Y., 2014. Methods for assessing the spatial distribution and dynamics of radiocesium in tree components in forest ecosystems (in Japanese). Bull. For. For. Prod. Res. Inst. 13, 113–136.
Katata, G., Chino, M., Kobayashi, T., Terada, H., Ota, M., Nagai, H., Kajino, M., Draxler, R., Hort, M., Malo, A., et al., 2015. Detailed source term estimation of the atmospheric release for the Fukushima Daiichi Nuclear Power Station accident by coupling simulations of an atmospheric dispersion model with an improved deposition scheme and oceanic dispersion model. Atmos. Chem. Phys. 15, 1029–1070. https://doi.org/10.5194/acp-15-1029-2015.
Kato, H., Onda, Y., Hisadome, K., Loffredo, N., Kawamori, A., 2017. Temporal changes in radiocesium deposition in various forest stands following the Fukushima Dai-ichi Nuclear Power Plant accident. J. Environ. Radioact. 166, 449–457. https://doi.org/10.1016/j.jenvrad.2015.04.016.
Kirchner, G., 1998. Applicability of compartmental models for simulating the transport of radionuclides in soil. J. Environ. Radioact. 38, 339–352. https://doi.org/10.1016/S0265-931X(97)00035-0.
Komatsu, M., Hirai, K., Nagakura, J., Noguchi, K., 2017. Potassium fertilisation reduces radiocesium uptake by Japanese cypress seedlings grown in a stand contaminated by the Fukushima Daiichi nuclear accident. Sci. Rep. 7, 15612. https://doi.org/10.1038/s41598-017-15401-w.
Komatsu, M., Kaneko, S., Ohashi, S., Kuroda, K., Sano, T., Ikeda, S., Saito, S., Kiyono, Y., Tonosaki, M., Miura, S., et al., 2016. Characteristics of initial deposition and behavior of radiocesium in forest ecosystems of different locations and species affected by the Fukushima Daiichi Nuclear Power Plant accident. J. Environ. Radioact. 161, 2–10. https://doi.org/10.1016/j.jenvrad.2015.09.016.
Linkov, I., Burmistrov, D., Kandlikar, M., Schell, W., 1999. Reducing uncertainty in the radionuclide transport modeling for the Chernobyl forests using bayesian updating. In: Contaminated Forests. Springer, pp. 143–150.
Loffredo, N., Onda, Y., Hurtevent, P., Coppin, F., 2015. Equation to predict the ^{137}Cs leaching dynamic from evergreen canopies after a radio-cesium deposit. J. Environ. Radioact. 147, 100–107. https://doi.org/10.1016/j.jenvrad.2015.05.018.
Loffredo, N., Onda, Y., Kawamori, A., Kato, H., 2014. Modeling of leachable ^{137}Cs in throughfall and stemflow for Japanese forest canopies after Fukushima Daiichi Nuclear Power Plant accident. Sci. Total Environ. 493, 701–707. https://doi.org/10.1016/j.scitotenv.2014.06.059.
Mahara, Y., Ohta, T., Ogawa, H., Kumata, A., 2014. Atmospheric direct uptake and long-term fate of radiocesium in trees after the Fukushima nuclear accident. Sci. Rep. 4. https://doi.org/10.1038/srep07121.
Marjoram, P., Molitor, J., Plagnol, V., Tavaré, S., 2003. Markov chain Monte Carlo without likelihoods. Proc. Natl. Acad. Sci. U.S.A. 100, 15324–15328. https://doi.org/10.1073/pnas.0306899100.
Morino, Y., Ohara, T., Nishizawa, M., 2011. Atmospheric behavior, deposition, and budget of radioactive materials from the Fukushima Daiichi nuclear power plant in march 2011. Geophys. Res. Lett. 38.
Nagakura, J., Abe, H., Zhang, C., Takano, T., Masamichi, T., 2016. Cesium, rubidium and potassium content in the needles and wood of Japanese cedar trees harvested from the sites of different radiocesium deposition levels (in Japanese). Jpn. J. For. Environ. 58, 51–59.
Nakanishi, T., Matsunaga, T., Koarashi, J., Atarashi-Andoh, M., 2014. ^{137}Cs vertical migration in a deciduous forest soil following the Fukushima Dai-ichi Nuclear Power Plant accident. J. Environ. Radioact. 128, 9–14. https://doi.org/10.1016/j.jenvrad.2013.10.019.
Niizato, T., Abe, H., Mitachi, K., Sasaki, Y., Ishii, Y., Watanabe, T., 2016. Input and output budgets of radiocesium concerning the forest floor in the mountain forest of Fukushima released from the TEPCO's Fukushima Dai-ichi nuclear power plant accident. J. Environ. Radioact. 161, 11–21. https://doi.org/10.1016/j.jenvrad.2016.04.017.
Nishikiori, T., Watanabe, M., Koshikawa, M.K., Takamatsu, T., Ishii, Y., Ito, S., Takenaka, A., Watanabe, K., Hayashi, S., 2015. Uptake and translocation of radiocesium in cedar leaves following the Fukushima nuclear accident. Sci. Total Environ. 502, 611–616. https://doi.org/10.1016/j.scitotenv.2014.09.063.
Nishina, K., Hayashi, S., 2015. Modeling radionuclide Cs and C dynamics in an artificial forest ecosystem in Japan FoRothCs ver1.0. Front. Environ. Sci. 3, 61. https://doi.org/10.3389/fenvs.2015.00061.
Ohashi, S., Kuroda, K., Takano, T., Suzuki, Y., Fujiwara, T., Abe, H., Kagawa, A., Sugiyama, M., Kubojima, Y., Zhang, C., Yamamoto, K., 2017. Temporal trends in ^{137}Cs concentrations in the bark, sapwood, heartwood, and whole wood of four tree species in Japanese forests from 2011 to 2016. J. Environ. Radioact. 178–179, 335–342. https://doi.org/10.1016/j.jenvrad.2017.09.008.
Ota, M., Nagai, H., Koarashi, J., 2016. Modeling dynamics of ^{137}Cs in forest surface environments: application to a contaminated forest site near Fukushima and assessment of potential impacts of soil organic matter interactions. Sci. Total Environ. 551, 590–604. https://doi.org/10.1016/j.scitotenv.2016.02.068.
Pröhl, G., Ehlken, S., Fiedler, I., Kirchner, G., Klemt, E., Zibold, G., 2006. Ecological half-lives of ^{90}Sr and ^{137}Cs in terrestrial and aquatic ecosystems. J. Environ. Radioact. 91, 41–72. https://doi.org/10.1016/j.jenvrad.2006.08.004.
R Core Team, 2017. R: a Language and Environment for Statistical Computing. R Foundation for Statistical Computing, Vienna, Austria URL. https://www.R-project.org/.
Rantavaara, A., Vetikko, V., Raitio, H., Aro, L., 2012. Seasonal variation of the ^{137}Cs level and its relationship with potassium and carbon levels in conifer needles. Sci. Total Environ. 441, 194–208. https://doi.org/10.1016/j.scitotenv.2012.09.045.
Rigol, A., Vidal, M., Rauret, G., 2002. An overview of the effect of organic matter on soil–radiocaesium interaction: implications in root uptake. J. Environ. Radioact. 58, 191–216. https://doi.org/10.1016/S0265-931X(01)00066-2.
Shaw, G., 2007. Radionuclides in forest ecosystems. Radioactiv. Environ. 10, 127–155. https://doi.org/10.1016/S1569-4860(06)10006-6.
Shaw, G., Venter, A., Avila, R., Bergman, R., Bulgakov, A., Calmon, P., Fesenko, S., Frissel, M., Goor, F., Konoplev, A., et al., 2005. Radionuclide migration in forest ecosystems–results of a model validation study. J. Environ. Radioact. 84, 285–296. https://doi.org/10.1016/j.jenvrad.2003.09.006.
Soetaert, K., Herman, P.M., 2008. A Practical Guide to Ecological Modelling: Using R as a Simulation Platform. Springer Science & Business Media.
Spiridonov, S., Fesenko, S., Sanzharova, N., 2005. Modelling of ^{137}Cs behaviour in the soil-plant system following the application of ameliorants. Radioprotection 40, S119–S124.
Tagami, K., Uchida, S., 2015. Effective half-lives of ^{137}Cs from persimmon tree tissue parts in Japan after Fukushima Dai-ichi Nuclear Power plant accident. J. Environ. Radioact. 141, 8–13. https://doi.org/10.1016/j.jenvrad.2014.11.019.
Takada, M., Yasutaka, T., Okuda, T., 2016. Simplified measurement method for dissolved radio-Cs in litter and soil seepage water using copper-substituted Prussian blue. Chemosphere 163, 234–241. https://doi.org/10.1016/j.chemosphere.2016.08.010.
Thiry, Y., Albrecht, A., Tanaka, T., 2018. Development and assessment of a simple ecological model (TRIPS) for forests contaminated by radiocesium fallout. J. Environ. Radioact. 190–191, 149–159. https://doi.org/10.1016/j.jenvrad.2018.05.009.
Thiry, Y., Garcia-Sanchez, L., Hurtevent, P., 2016. Experimental quantification of radiocesium recycling in a coniferous tree after aerial contamination: field loss dynamics, translocation and final partitioning. J. Environ. Radioact. 161, 42–50. https://doi.org/10.1016/j.jenvrad.2015.12.017.
Thiry, Y., Goor, F., Riesen, T., 2002. The true distribution and accumulation of radiocaesium in stem of Scots pine (*Pinus sylvestris* L.). J. Environ. Radioact. 58, 243–259. https://doi.org/10.1016/S0265-931X(01)00068-6.
Vrugt, J.A., Sadegh, M., 2013. Toward diagnostic model calibration and evaluation: approximate bayesian computation. Water Resour. Res. 49, 4335–4345. https://doi.org/10.1002/wrcr.20354.
Wegmann, D., Leuenberger, C., Excoffier, L., 2009. Efficient approximate Bayesian computation coupled with Markov chain Monte Carlo without likelihood. Genetics 182, 1207–1218. https://doi.org/10.1534/genetics.109.102509.
Wei, L., Kinouchi, T., Yoshimura, K., Velleux, M.L., 2017. Modeling watershed-scale ^{137}Cs transport in a forested catchment affected by the Fukushima Dai-ichi Nuclear Power Plant accident. J. Environ. Radioact. 171, 21–33. https://doi.org/10.1016/j.jenvrad.2017.01.017.
Yoschenko, V., Takase, T., Hinton, T.G., Nanba, K., Onda, Y., Konoplev, A., Goto, A., Yokoyama, A., Keitoku, K., 2017. Radioactive and stable cesium isotope distributions and dynamics in Japanese cedar forests. J. Environ. Radioact. https://doi.org/10.1016/j.jenvrad.2017.09.026.